Inorganic Chemistry

Article

pubs.acs.org/IC

Structure and Chemistry of $SeF_x(CN)_{4-x}$ Compounds

Stefanie Fritz, Christian Ehm,*[,†] and Dieter Lentz

Institut für Chemie und Biochemie, Anorganische Chemie, Freie Universität Berlin, Fabeckstrasse 34/36, 14195 Berlin, Germany

Supporting Information

ABSTRACT: Several new $SeF_2(CN)_2$–donor complexes with N or O based donor molecules are reported. Due to orbital overlap effects 12-crown-4 (1,4,7,10-tetraoxacyclododecane) shows unsymmetric ether oxygen coordination. Solvent coordination (secondary bonding interactions, SBI) in $SeF_x(CN)_{4-x}$ compounds is weak and does not influence decomposition pathways (neutral and anionic). Barriers for decomposition are relatively high in $SeF_2(CN)_2$ but decrease significantly in compounds with higher cyanide content. In the presence of fluoride ions, facile substitution pathways exist; however, reductive elimination is also favored. In the absence of fluoride ions decomposition barriers are higher, but so are substitution barriers (σ-metathesis). Therefore, successful isolation of $Se(CN)_4$ appears to be significantly hampered. In addition, previously unknown trifluoromethyliminoseleniumdifluoride was cleanly synthesized utilizing the instability of $SeF(CN)_3$ toward reductive FCN elimination (preferred over the thermodynamically favored NCCN elimination) and subsequent FCN incorporation to SeF_4 through double F-migration.

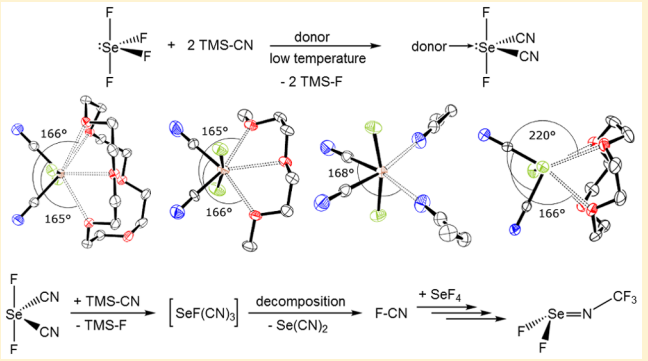

1. INTRODUCTION

In the course of our studies of pseudohalogen compounds of the chalcogens, we became interested in selenium tetracyanide, Scheme 1.

Scheme 1. VSEPR Structures of Selenium Tetracyanide and Selenium Difluoride Dicyanide

For a long time the only known homoleptic selenium cyanides were low valent $Se_3(CN)_2$, $Se_2(CN)_2$, and $Se(CN)_2$.[1−4] Their X-ray crystal structures were redetermined in 2006 and 2008.[5,6] Klapötke et al. reported an unsuccessful attempt to synthesize $Se(CN)_4$ and attributed its instability to the large exothermicity of its reductive decomposition into $Se(CN)_2$ and cyanogen (−71.8 kcal/mol, MP2 level of theory). While this without doubt represents a strong thermodynamic driving force for decomposition, it does not exclude the possibility that the barrier for such a reaction is not sufficiently high to permit isolation of a metastable molecule at low temperature. Furthermore, reaction intermediates could be unstable, and the observation of the decomposition products is therefore not unambiguous proof for the intermediate existence of $Se(CN)_4$.

Stabilization of chalcogen compounds can be achieved through secondary bonding interactions (SBI) as observed in the case of selenium dibromide and dichloride or $Te(CN)_4$.[7−10]

$Te(CN)_4$, first reported by Klapötke et al. and characterized by Raman spectroscopy,[7] could be successfully stabilized using coordinating solvents. In 2008, we presented the first selenium cyanide with selenium in the oxidation state IV, $SeF_2(CN)_2$.[11] The congeneric sulfur dicyanide difluoride was only poorly characterized.[12]

We originally planned to use coordinating solvents to stabilize the elusive $Se(CN)_4$ species and obtain its crystal structure. However, unlike its heavier congener $Te(CN)_4$, the selenium derivative could not be successfully isolated, even at very low temperatures. We now describe our investigations of these systems using experimental and computational tools to gain insight into the chemistry of mixed selenium(IV) fluoride cyanide complexes as well as $Se(CN)_4$. Additionally, we clarify the decomposition mechanisms of selenium(IV) cyanides of the type $SeF_x(CN)_{4-x}$ both in the presence and absence of fluoride ions and the influence of solvents on these mechanisms. Intermediates of the type $SeF_x(CN)_{4-x}$, including the aforementioned $SeF_2(CN)_2$, feature a rich chemistry, as exemplified by their redox behavior, intermolecular equilibria, secondary bonding interactions, and fluorocyan incorporation.

2. EXPERIMENTAL SECTION

All reactions were carried out using Schlenk techniques in carefully dried PFA tubes (PFA = perfluoro-alkoxypolymer) either under vacuum or an argon atmosphere. If not stated otherwise, crystals were grown in 6.5 mm PFA tubes, and NMR measurements were performed in 3 mm (inner diameter) PFA tubes. Volatile reagents were condensed into the reaction tube using a glass vacuum line system with Teflon Normag or J. Young valves. Solvents were carefully

Received: January 15, 2015
Published: May 12, 2015

DOI: 10.1021/acs.inorgchem.5b00107
Inorg. Chem. 2015, 54, 5220−5231

dried and distilled onto molecular sieves for storage. THF was stored over sodium−potassium alloy and directly condensed into the reaction vessel. The following reagents were handled in a drybox (MBraun): SeF_4, prepared according to literature procedure;[13] TMSCN (Me_3SiCN, Acros) and 12-crown-4 (Sigma-Aldrich), distilled; and 18-crown-6 (1,4,7,10,13,16-hexaoxacyclooctadecane) (Sigma-Aldrich), sublimed. ^{13}C-labeled $Me_3Si^{13}CN$ was synthesized via metathesis from Me_3SiCl (Sigma-Aldrich) and $K^{13}CN$ (eurisotop) and purified via fractional distillation.

$SeF_2(CN)_2$−Donor Complexes for X-ray Analysis. *$SeF_2(CN)_2$(diglyme).* SeF_4 (150 mg, 0.96 mmol) was dissolved in a mixture of diglyme (bisethylene glycoldimethyl ether) (250 mg, 1.87 mmol) and toluene (0.8 mL) in a PFA tube. After the reaction mixture was cooled to −196 °C and evacuated, Me_3SiCN (193 mg, 1.95 mmol) was condensed into the tube using a glass vacuum line system and the tube subsequently flame-sealed. The reaction mixture then was allowed to warm to −10 °C for a few seconds to dissolve solid Me_3SiCN, held at −60 °C for 10 min, and stored at −80 °C. After 20 days colorless rectangular crystals had formed. CCDC: 1034967. Raman (−90 °C): $\tilde{\nu}$ (relative intensity) = 83 (100), 101 (45), 136 (72), 157 (87), 218 (9), 248 (16), 287 (8), 320 (7), 338 (10), 386 (6), 411 (7), 422 (16), 472 (73), 485 (58), 523 (55), 532 (62), 578 (17), 619 (4), 666 (2), 695 (4), 786 (8), 835 (6), 857 (25), 945 (2), 1002 (10), 1011 (3), 1024 (7), 1066 (6), 1091 (2), 1129 (5), 1141 (4), 1159 (4), 1211 (2), 1234 (4), 1244 (4), 1273 (6), 1284 (4), 1377 (4), 1397 (2), 1428 (2), 1441 (7), 1452 (7), 1471 (9), 1486 (3), 1602 (2), 2087 (1), 2201 (17), 2834 (7), 2864 (3), 2883 (4), 2904 (6), 2928 (6), 2945 (8), 3003 (3), 3055 (2) cm^{-1}.

$SeF_2(CN)_2(THF)_2$. THF (0.5 mL) was condensed onto SeF_4 (162 mg, 1.05 mmol) in a PFA tube and allowed to warm to ambient temperature to dissolve SeF_4. The solution was cooled to −196 °C again, and Me_3SiCN (205 mg, 2.07 mmol) was condensed into the tube which subsequently was flame-sealed. The reaction mixture was shaken at −70 °C to dissolve solid Me_3SiCN and slowly cooled to −80 °C within 12 h. Very temperature labile colorless needle-shaped crystals were obtained. The single crystal decomposed very fast during X-ray data collection due to a failure in the cooling system, resulting in a θ_{full} of only 0.48. CCDC: 1034969.

$SeF_2(CN)_2$(18-crown-6). A solution of 18-crown-6 (18 mg, 0.07 mmol) in toluene (0.3 mL) was added to SeF_4 (11 mg, 0.07 mmol) in a PFA tube. While the stirred mixture was cooled to −40 °C a solution of Me_3SiCN (10 mg, 0.10 mmol) in toluene (0.2 mL) was added, and the reaction mixture was stirred for 1 h at −25 °C. The tube was cooled to −196 °C, evacuated, and flame-sealed. After 100 days at −58 °C small colorless rhombohedral crystals were obtained. CCDC: 1034966.

$SeF_2(CN)_2$(12-crown-4)·toluene. While the reaction mixture was cooled to to −60 °C, a solution of Me_3SiCN (62 mg, 0.63 mmol) in toluene (0.3 mL) was added to a stirred mixture of SeF_4 (46 mg, 0.30 mmol), 12-crown-4 (60 mg, 0.34 mmol), and toluene (0.5 mL). The reaction mixture was cooled to −196 °C and the PFA-tube flame-sealed. Warming to −60 °C gave a clear solution. Very slow cooling to −80 °C within 2 days resulted in formation of colorless platelets. CCDC: 1034965. Raman (−90 °C): $\tilde{\nu}$ (relative intensity) = 84 (85), 95 (100), 129 (68), 167 (81), 220 (21), 252 (18), 263 (11), 287 (9), 312 (7), 352 (12), 370 (10), 412 (26), 474 (51), 487 (60), 509 (17), 520 (26), 531 (36), 538 (61), 567 (12), 579 (12), 620 (12), 786 (36), 798 (26), 816 (13), 843 (3), 903 (8), 1002 (45), 1029 (16), 1041 (76), 1071 (5), 1090 (4), 1115 (5), 1141 (5), 1155 (6), 1178 (6), 1210 (10), 1248 (5), 1257 (6), 1292 (9), 1378 (5), 1387 (5), 1446 (12), 1460 (14), 1584 (6), 1604 (9), 2175 (1), 2203 (10), 2871 (8), 2886 (8), 2916 (10), 2939 (14), 2966 (7), 3037 (4), 3053 (8) cm^{-1}.

$SeF_2(CN)_2(EtCN)_2$. SeF_4 (168 mg, 1.08 mmol) was dissolved in propionitrile (EtCN) (2.0 mL). The stirred solution was cooled to −78 °C, and a solution of Me_3SiCN (158 mg, 1.59 mmol) in propionitrile (0.5 mL) was added. After the reaction mixture was stirred for 5 h at −20 °C, volatile byproducts and three-fourths of the solvent were removed in vacuo. The resulting residue was redissolved at ambient temperature and crystallized by very slow cooling to −78 °C within 5 days. CCDC: 1034968. Raman (−90 °C): $\tilde{\nu}$ (relative intensity) = 84 (61), 94 (67), 107 (65), 125 (76), 165 (100), 221 (45), 229 (44), 247 (24), 287 (23), 391 (23), 419 (26), 478 (61), 497 (60), 537 (92), 583 (19), 618 (41), 693 (4), 758 (5), 791 (7), 837 (36), 1002 (25), 1073 (21), 1261 (10), 1312 (7), 1379 (4), 1411 (5), 1426 (12), 1435 (14), 1459 (17), 2179 (1), 2209 (20), 2246 (26), 2258 (54), 2742 (2), 2846 (3), 2894 (13), 2912 (10), 2944 (42), 2972 (19), 2997 (13) cm^{-1}.

$Se(CN)_2$(18-crown-6)·$^1/_2$ 18-crown-6. Crystals for X-ray analysis were obtained from a NMR sample: a solution of 18-crown-6 (39 mg, 0.15 mmol) in d_8-THF (0.3 mL) was added via Schlenk techniques to SeF_4 (25 mg, 0.16 mmol) in a PFA tube. After the reaction mixture was cooled to −196 °C and evacuated, $TMS^{13}CN$ (51 mg, 0.51 mmol) was condensed into the tube which was subsequently sealed and shaken. After the sample was left for 2 h at −78 °C followed by 2 days at −30 °C, small pale yellow crystals formed on the existing precipitate. CCDC: 1034964.

As all compounds are highly air, moisture, and temperature sensitive, crystal selection and mounting must be performed at low temperature using equipment similar to that described in the literature.[14] Crystallizing $SeF_2(CN)_2$ from THF is the most difficile experiment described here for the following reasons: (1) Crystallization experiments require a highly concentrated solution of $SeF_2(CN)_2$ in THF for a sufficient crystallization rate, but this in turn leads to faster decomposition due to higher internal thermal energy (originating from the initial reaction). Thus, a very precise balanced concentration−cooling system is needed. (2) Preparation of the crystals for the X-ray measurement is nontrivial as they form thin needles which are extremely sensitive to loss of THF and, if not thick enough, do not "survive" the preparation procedure. We were able to reproduce crystallization but not able to obtain another X-ray data set, regretfully. CCDC 1034964−1034969 contain the supplementary crystallographic data for this Article. These data can be obtained free of charge from The Cambridge Crystallographic Data Centre via www.ccdc.cam.ac.uk/data_request/cif.

NMR Procedures. *$SeF_2(^{13}CN)_2$.* In a typical NMR experiment SeF_4 (0.25 mmol) was dissolved in the appropriate deuterated solvent (approximately 0.2−0.3 mL) in a PFA NMR tube. After 2 equiv (0.5 mmol) of $Me_3Si^{13}CN$ were condensed into the frozen solution the tube was flame-sealed, shaken, and handled at low temperatures (maximum −60 °C, depending on the solubility of $Me_3Si^{13}CN$). NMR data are summarized in Table 4. All spectra were recorded at −80 °C and referenced to Me_4Si (^{13}C, 101 MHz), $CFCl_3$ (^{19}F, 376 MHz), or Me_2Se (^{77}Se, 76 MHz), respectively.

Decomposition. Two decomposition experiments were carried out with different amounts of $TMS^{13}CN$. The byproduct TMSF (trimethylsilyl fluoride) was used as internal standard to evaluate the amounts of fluorinated compounds. Not explicitly given NMR values can be obtained from literature.[11]

In the first experiment, 2 equiv of the cyanide were used in a DME/d_8-toluene mixture to produce pure $SeF_2(^{13}CN)_2$ with only small impurities of $Se(^{13}CN)_2$ and $(^{13}CN)_2$. Decomposition was provoked by warming the sample to room temperature (15 min), followed by cooling to −80 °C to stop decomposition. This resulted in a higher amount of $Se(^{13}CN)_2$, less $SeF_2(^{13}CN)_2$ and the appearance of signals for $F^{13}CN$, SeF_4, and $F_2Se{=}N{-}^{13}CF_3$ and a few other signals (unidentified but $^{13}CF_3$-group containing). Repetition of this procedure increases the amounts of $F_2Se{=}N{-}^{13}CF_3$ and $Se(^{13}CN)_2$ while the amount of $SeF_2(^{13}CN)_2$ decreases. After 5 h at room temperature $SeF_2(^{13}CN)_2$ was fully decomposed, and the initially clear colorless solution turned yellow.

The second experiment (1.7 equiv of $TMS^{13}CN$ in d_5-propionitrile) resulted in formation of $SeF_2(^{13}CN)_2$ plus remaining SeF_4. After decomposition (6 h at room temperature), $F_2Se{=}N{-}^{13}CF_3$ and $Se(^{13}CN)_2$ were obtained as main products, and a small amount of SeF_4 remained. Using less than 2 equiv of $TMS^{13}CN$ produces fewer unidentified $^{13}CF_3$-groups.

$F^{13}CN$. $\delta(^{19}F)$ (DME/C_7D_8, −80 °C, 376 MHz) = −154.3 (d, $^1J(^{19}F{-}^{13}C)$ = 419 Hz) ppm. $\delta(^{13}C\{^1H\})$ (DME/C_7D_8, −80 °C, 101 MHz) = 104.2 (d, $^1J(^{13}C{-}^{19}F)$ = 419 Hz) ppm.

DOI: 10.1021/acs.inorgchem.5b00107
Inorg. Chem. 2015, 54, 5220−5231

Table 1. Bond Parameters of $SeF_2(CN)_2$ Complexes

	diglyme	2 × THF	18-crown-6	12-crown-4	2 × EtCN
Se—D_{min}	2.658 (3)	2.596 (6)	2.7593 (9)	2.868 (2)	2.750 (1)
Se—D_{max}	2.848 (3)		3.0878 (9)	3.024 (2)	
Se—F1	1.838 (2)	1.821 (8)	1.8429 (8)	1.829 (1)	1.8376 (8)
Se—F2	1.829 (2)	1.822 (8)	1.8375 (8)	1.846 (2)	
F—Se—F	167.1 (1)	167.5 (4)	161.02 (4)	159.99 (7)	166.69 (5)
Se—C1	1.876 (3)	1.882 (9)	1.896 (1)	1.910 (3)	1.890 (1)
Se—C2	1.892 (3)		1.898 (1)	1.892 (3)	
C—Se—C	90.6 (2)	94.0 (5)	92.91 (6)	92.9 (1)	92.85 (7)
C≡N	1.137 (5)	1.14 (1)	1.150(2)	1.138 (3)	1.141 (2)
C≡N	1.121 (5)		1.142 (2)	1.141 (3)	
Se—C≡N	177.7 (3)	176.4 (8)	179.2 (1)	176.8 (3)	179.4 (1)
Se—C≡N	178.7 (4)		179.5 (1)	177.7 (2)	

$F_2Se{=}N{-}^{13}CF_3$. $\delta(^{77}Se\{^1H\})$ (C_2D_5CN, −80 °C, 76 MHz) = 1212 (tm, $^1J(^{77}Se{-}^{19}F)$ = 692 Hz) ppm; $\delta(^{19}F)$ (C_2D_5CN, −80 °C, 376 MHz) = 2.3 (s, F_2Se, $^1J(^{19}F{-}^{77}Se)$ = 692 Hz), −41.9 (d, $F_3{}^{13}C$, $^1J(^{19}F{-}^{13}C)$ = 260 Hz) ppm. $\delta(^{13}C\{^1H\})$ (C_2D_5CN, −80 °C, 101 MHz) = 123.6 (q, $^1J(^{13}C{-}^{19}F)$ = 260 Hz) ppm. $\delta(^{19}F)$ (DME/C_7D_8, −80 °C, 376 MHz) = −3.9 (s, F_2Se, $^1J(^{19}F{-}^{77}Se)$ = 640 Hz), −40.7 (dt, $F_3{}^{13}C$, $^1J(^{19}F{-}^{13}C)$ = 262 Hz, $^3J(^{19}F{-}^{19}F)$ = 11.6 Hz) ppm.

Computational Details. All compounds were fully optimized using the Gaussian 09 software package[15] at the density functional level of theory employing the Becke, three parameter, Lee−Yang−Parr exchange correlation functional (B3LYP) in combination with the internally stored 6-311+G(d,p) basis set.[16−20] Thermochemical corrections were derived at this level (298 K, enthalpy and entropy). Single point (SP) calculations to determine final energies were then done at the M06-2X[21] and TPSSh-D0[22] level of theory employing polarized valence-triple ζ (Dunning) basis sets,[23−30] from the EMSL basis set exchange library,[31,32] with aug-cc-pVTZ quality. Grimme's dispersion correction[33,34] was included via the standalone dftd3 program using the "-zero" option to invoke zero damping (only for coordination energies but not for transition states as TS geometries can lead to artificial overcorrection).[35]

All structures represent either true minima (as indicated by the absence of imaginary frequencies) or transition states (with exactly one imaginary frequency corresponding to the reaction coordinate). Geometry calculations and single point calculations were performed at the standard Gaussian 09 quality settings [Scf=Tight and Int(Grid=Fine)] except where noted otherwise in the Supporting Information. In simple cases, transition states were located using a suitable guess and the Berny algorithm[36] (Opt=TS). For more complex cases, we used either the Synchronous Transit-Guided Quasi-Newton (STQN) Method, developed by H. B. Schlegel and co-workers[37,38] (Opt=QST2 or QST3), or a relaxed potential energy scan to arrive at a suitable transition state guess, followed by a quasi-Newton or eigenvector-following algorithm to complete the optimization.

Contributions from basis set superposition errors (BSSEs) to all coordination energies have been estimated by Boys and Bernardi's counterpoise procedure[39] as implemented in Gaussian 09. BSSE contributions were assumed to be constant from the solvent coordinated complex on for two reasons: (a) the TS geometries are close to the geometries of the solvent complexes; (b) a counterpoise correction requires consistent assignment of atoms to fragments, which is not possible when different reaction types (e.g., FCN and NCCN elimination) starting from the same species are considered.

Solvent influence (diethyl ether, ε = 4.24) was modeled using the polarizable continuum model (PCM) implemented in the Gaussian 09 software suite, and all structures were reoptimized with the PCM model.[40]

3. RESULTS AND DISCUSSION

Secondary Bonding Interactions in $SeF_2(CN)_2$−Donor Complexes. During our survey we obtained X-ray crystal structures of a series of different adducts of the thermally unstable $SeF_2(CN)_2$, with oxygen- as well as nitrogen-donor molecules, in particular bisethylene glycoldimethyl ether (diglyme), tetrahydrofuran (THF), 18-crown-6, 12-crown-4, and propionitrile (EtCN).

In principle, coordination of donor-molecules is very similar among the studied compounds (Table 1, Figures 1−3) and

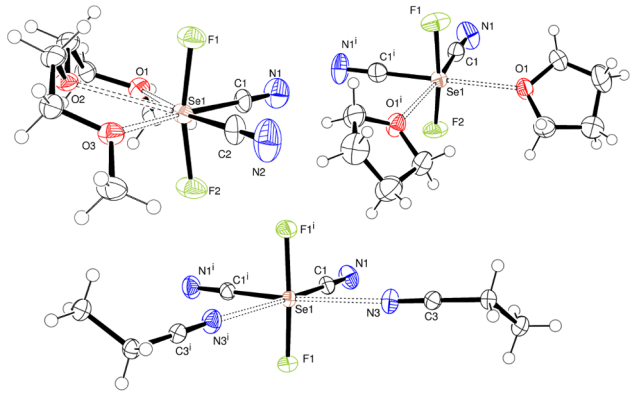

Figure 1. Molecular structures of $SeF_2(CN)_2$ adducts: (top left) diglyme, (top right) bis-tetrahydrofuran, (bottom) bis-propionitrile. ORTEP[41] drawing with 50% probability ellipsoids.

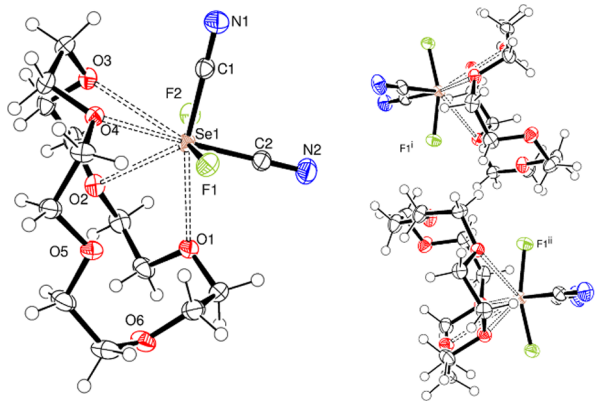

Figure 2. Molecular structure of $SeF_2(CN)_2$·18-crown-6, left: single molecule. Right: orientation of the intermolecular F−H-contacts parallel to the *c*-axis. ORTEP[41] drawing with 50% probability ellipsoids.

DOI: 10.1021/acs.inorgchem.5b00107
Inorg. Chem. 2015, 54, 5220−5231

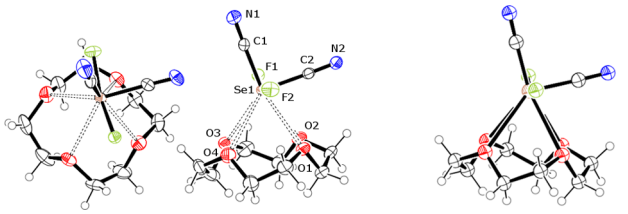

Figure 3. Left: solid state structure of $SeF_2(CN)_2$·12-crown-4·toluene. Two molecules are linked via secondary N2−Se1 contact of 3.39 Å in the direction of the *b*-axis (as it has no influence, cocrystallized toluene is not shown). ORTEP[41] drawing with 50% probability ellipsoids. Right: calculated gas phase structure of $SeF_2(CN)_2$·12-crown-4.

comparable to that of the 1,2-dimethoxyethane adduct.[11] The $SeF_2(CN)_2$ fragment forms a Ψ-trigonal bipyramid with C_{2v}-symmetry in line with VSEPR theory, and 2−4 donor atoms coordinate opposite to the cyanide groups.

Cyanide groups are located in the equatorial plane with bond angles for all five complexes between 90° and 94°, with the adducts of diglyme and tetrahydrofuran representing both extremes (Scheme 2, Figure 1). Compared to the other known

Scheme 2. Formation of $SeF_2(CN)_2$

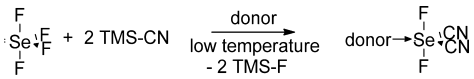

examples of selenium(IV) fluorides (Table 2), these angles are quite small and far away from the ideal equatorial plane angle of 120° presumably due to a much higher p-character of the equatorial hybrid orbital. Axial fluorine atoms are bent in the direction of the cyanide groups resulting in F−Se−F bond angles 160−168° in the 12-crown-4 and tetrahydrofuran adducts, respectively, which is in between the other known examples.[42−45] Se−F and Se−C bond lengths match the expected range, the averaged 0.1 Å shorter Se−C bond length in $SeF_2(CN)_2$ compared to $SeF_2(CF_3)_2$ is caused by the difference in carbon orbitals used to form the Se−C bond (sp vs sp^3).

Distances between donor atoms and selenium (Table 1) are about 10−20% below the sum of the van der Waals radii.[46] Coordination of two molecules in the equatorial plane is observed for monodentate donors, while diglyme uses all three oxygen atoms for coordination (Figure 1) with the middle O(2)−Se distance being 1.5 Å longer than the terminal ones. Four oxygen atoms participate in complex formation in the crown ether adducts. 18-Crown-6 coordinates unsymmetrically with one oxygen atom (O1) in the equatorial plane, two oxygen atoms (O3 and O4) almost exactly above and below the equatorial plane, and the remaining oxygen atom (O2) in a plane spanned by the selenium and fluorine atoms (Figure 2). As a result the crown ether deflects in a manner forming two intermolecular hydrogen contacts to a fluorine atom of an adjacent $SeF_2(CN)_2$ molecule.

Although 12-crown-4 can be viewed as two bridged 1,2-dimethoxyethane molecules, the resulting SBI-coordination is quite different. The coordination of two oxygen atoms above and below the equatorial plane, respectively, is similar to the already published 1,2-dimethoxyethane adduct.[11] However, due to the strain in the cyclic ether the crown is tilted in the direction of one of the cyanide groups. Consequently, a weak solid state ("second order") N−Se interaction is observed between adjacent $SeF_2(CN)_2$ molecules (Figure 3) with a distance of 3.39 Å which is only 0.06 Å below the sum of the van der Waals radii.[46]

Interestingly, the distorted coordination of the 12-crown-4-molecule is also observed in the calculated gas phase structure (Figure 3, right), where no "second order" interaction can play a role. Therefore, the distorted coordination of the crown ether is not a packing effect enforced by "second order" interactions but the "second order" interaction appears to be a crystal packing effect. Thus, $SeF_2(CN)_2$·12-crown-4 still shows characteristics of the supposed crystal structure of pure, noncoordinated $SeF_2(CN)_2$ which is expected to have intermolecular SeCN−Se contacts.

Inspection of the HOMO of $SeF_2(CN)_2$ and the LUMO of 12-crown-4 (Figure 4) leads to more detailed insights: the cyclic ether is too strained to achieve two ideal orbital overlaps between one orbital lobe of $SeF_2(CN)_2$ and the lone pairs of two oxygen atoms, respectively. Apparently, one accurate matching overlap is favored over two partially matching overlaps. By contrast, 1,2-dimethoxyethane, which is just the split crown ether, can achieve two accurate orbital overlaps.

An analysis of the X-ray crystal structures of the different $SeF_2(CN)_2$ complexes gives evidence for a perfect coordination angle due to orbital overlap (Figure 5). It is approximately 166° between the Se−CN- and the Se−O/N-axis. If steric constraints arise (2 × DME), the angle widens to 177° due to unfavorable H−H interactions between the methyl groups of each donor molecule.

DFT calculations (Table 3) show that, even though coordination enthalpies for two DME molecules to Se(IV) and Se(II) species are high (−15 to −25 kcal/mol), the large entropic penalty from forming a supermolecule out of 3 or 4 independent molecules makes the formation of all coordination compounds endergonic at room temperature at the B3LYP level of theory. Dispersion corrections are necessary to describe this interaction sufficiently. However, even with dispersion corrections, coordination energies are only slightly (M06-2X) to moderately (TPSSh-D0) exergonic. At lower temperature the entropic penalty ($\Delta G = \Delta H - T\Delta S$) becomes smaller, and formation of $SeF_x(CN)_{4-x}$ species with two coordinated DME molecules becomes more favorable. In line with experimental data,[11] the gas phase structure predicts that the coordination space is "oversaturated" (two different Se−O distances, Figure 6).

The formation of a large supermolecule consisting of two $Se^{II}(CN)_2$ units and two bridging DME molecules, as

Table 2. Bond Parameters of $Se^{IV}F_2(R)_2$ Complexes (R = Equatorial Ligand, D = Donor Atom)

	Se−D [Å]	$Se-F_{ax}$ [Å]	F−Se−F [deg]	$Se-R_{eq}$ [Å]	R−Se−R [deg]
$SeF_2(CF_3)_2$[42]		1.83	158	2.02	119
$SeF_2(CN)_2$	2.60−3.09	1.82−1.85	160−168	1.88−1.91	91−94
SeF_4(s)[43,44]	2.65−2.66	1.79−1.80	169	1.67−1.68	97
SeF_4(g)[45]		1.77	169	1.68	101

DOI: 10.1021/acs.inorgchem.5b00107
Inorg. Chem. 2015, 54, 5220−5231

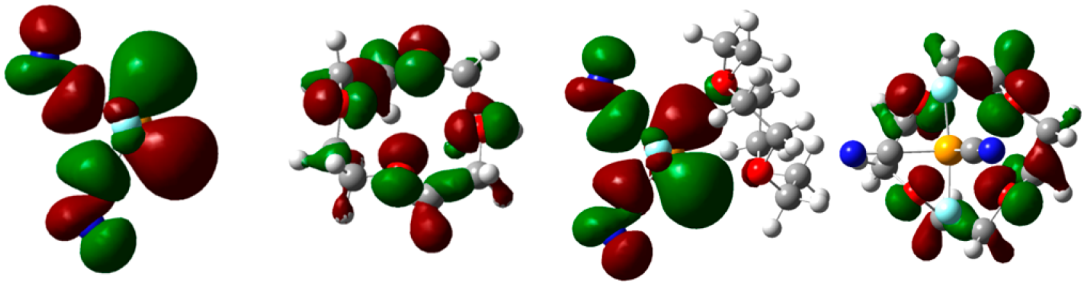

Figure 4. Visualization of calculated frontier orbitals. From left to right: LUMO of $SeF_2(CN)_2$ (viewing direction is F−Se−F, cyanide groups are in the paper plane, major expansions are in the elongation of each Se−CN bond, isovalue 0.02). HOMO of 12-crown-4 (major expansions are the lone pairs of the oxygen atoms, isovalue 0.04). LUMO complex (isovalue 0.02). HOMO complex (isovalue 0.04).

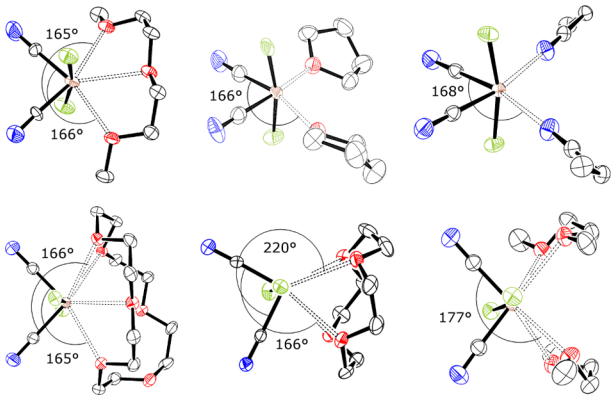

Figure 5. Analysis of the solid state structures of $SeF_2(CN)_2$ adducts with respect to coordination angles.[47]

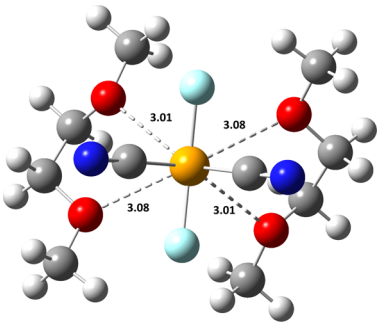

Figure 6. Coordination of two DME units at $Se^{IV}F_2(CN)_2$, calculated structure.

previously observed by us, is similarly barely or moderately exergonic at room temperature, depending on the level of theory.[11] Complexation enthalpies and Gibbs free energies for selenium(IV) compounds show a slight dependence on the substitution pattern, and become more exergonic with increasing cyanide content. This effect is relatively small (~3 kcal/mol per F/CN substitution); CN^- is a strong electron withdrawing pseudohalogen, but it does not have the same electronic features that fluorine has.

Overall, secondary bonding interactions between the Se atom and donor molecules are rather weak, in line with earlier findings by Panda and Behera.[48] Without strong binding of the donor molecules to selenium, it is questionable whether donors can have enough influence on the decomposition pathway(s) of $Se(CN)_4$ to allow for its successful isolation.

X-ray experiments indicate that the crown ethers stabilize $SeF_2(CN)_2$ very well. In THF, however, the formation of $SeF_2(CN)_2$ is faster, but crystals of the adducts are very sensitive toward the loss of coordinated THF and subsequent decomposition. The additional stability of crystals of donors like DME and crown ethers is likely a chelate effect. Propionitrile stabilizes $SeF_2(CN)_2$ similarly to crown ethers.

Table 3. Energies, Enthalpies, and Gibbs Free Energies (in kcal/mol) for the Formation of $Se^{IV}F_x(CN)_{4-x}$ Complexes with Two DME Molecules and of $(Se^{II}(X)_2{\cdot}dme)_2$-type Complexes According to the Following Reaction Schemes

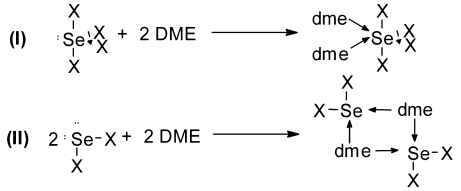

	Δ*E* (B3LYP)	Δ*H* (B3LYP)	Δ*G*(B3LYP)	Δ*G*(M06-2X)	Δ*G*(TPSSh-D0)
			Reaction (I)		
SeF_4	−18.4	−15.4	5.7	1.0	−3.3
SeF_3CN	−19.3	−16.2	5.6	−1.1	−5.4
$SeF_2(CN)_2$	−19.9	−16.7	5.5	−2.7	−7.3
$SeF(CN)_3$	−21.2	−17.9	4.5	−5.7	−10.9
$Se(CN)_4$	−22.8	−19.5	3.1	−10.2	−15.5
			Reaction (II)		
$2SeF_2$	−29.7	−24.9	9.9	3.4	−3.4
$2Se(CN)_2$	−20.4	−16.0	13.7	0.9	−5.8

DOI: 10.1021/acs.inorgchem.5b00107
Inorg. Chem. 2015, 54, 5220−5231

Additionally, fewer side products are experimentally observed in decomposition reactions due to the lower reactivity of nitriles toward selenium(IV) fluoride compounds compared to the cyclic ethers, which are vulnerable to ring opening and partial fluorination.

NMR Properties of $SeF_2(^{13}CN)_2$: Effect of Fluoride Traces. Effects of coordination of donor molecules are also observed in the NMR spectra. Interestingly, the ^{19}F NMR spectrum is far more solvent dependent than the ^{13}C NMR spectrum (Table 4). This is most likely induced by electronic effects of the solvent and its coordination ability.

Table 4. NMR Parameters of $SeF_2(^{13}CN)_2$ Complexes[a]

	d_8-toluene	DME/d_8-toluene	d_8-THF	CD_2Cl_2	d_5-propionitrile
ε (~rt)	2.38	7.3 (DME)	7.52	8.93	29.7
$\delta(^{19}F)$	−12.5 (s, broad)	−23.4 (t)	−32.5 (s, broad)	−32.5 (s, broad)	−35.7 (t)
$\delta(^{13}C)$	107 (t)	110 (t)	108.7 (t)	*b*	110 (t)
$^1J(^{77}Se-^{19}F)$	355	377	440	373	400
$^1J(^{77}Se-^{13}C)$	229	238	245	*b*	232
$^2J(^{19}F-^{13}C)$	17.7	19.2	15.7	*b*	16.6

[a]Chemical shifts referenced to external $CFCl_3$ (^{19}F; 376 MHz) or Me_4Si ($^{13}C\{^1H\}$; 101 MHz, −80 °C), respectively. Relative permittivity ε of the nondeuterated (protio) solvents at nearly room temperature (293−298 K; temperature dependency approximately linear). [b]Due to fast decomposition no ^{13}C NMR data is available.

The chemical shift can be expressed via the following equation

$$\delta = \delta_0 + \delta_S = \delta_0 + \delta_b + \delta_W + \delta_a + \delta_E \quad (1)$$

with δ_0 being the gas phase chemical shift and δ_S summarizing the solvent effects. Notable solvent effects are bulk susceptibility of the system δ_b, van der Waals interactions between solvent and solute δ_W, anisotropy of the solvent δ_a, and changes in the electric field due to the polarity of the dissolved molecules δ_E. In the case of $SeF_2(^{13}CN)_2$, the most important effects influencing the chemical shift are solvent−solute interactions (coordination, changes δ_W) and the pronounced differences in the permittivity of the solvents (changes δ_E). Both effects lead to an upfield shift as can be seen in Table 4.

The influence of the relative permittivity as main electronic effect is very high at small values of ε as indicated by the 20 ppm upfield shift in CD_2Cl_2 compared to d_8-toluene (both solvents do not coordinate strongly) but decreases at high values of ε. A logarithmic dependency is likely the best way to describe the correlation of the chemical shift and the relative permittivity.

The upfield shift caused by coordination is best illustrated by comparison of the measurements in CD_2Cl_2 and d_8-THF. The relative permittivity ε of dichloromethane exceeds THF by 1.4, yet chemical shifts are identical, due to the stronger coordination ability of THF. Consequently, the 11 ppm upfield shift obtained by addition of 1,2-dimethoxyethane to d_8-toluene is a synergetic effect of both the increasing permittivity and coordination ability.

Coupling constants differ by 85 Hz in the case of $^1J(^{77}Se-^{19}F)$ or 16 Hz in the case of $^1J(^{77}Se-^{13}C)$, respectively (Table 4), likely as a result of both electronic and coordination effects of the solvent,[49,50] but the latter effect is more pronounced. This can be understood by comparison of coupling constants in d_8-THF ($^1J(^{77}Se-^{19}F)$ = 440 Hz), d_5-propionitrile (400 Hz), and CD_2Cl_2 (373 Hz). The relative permittivity of propionitrile is an order of magnitude higher than THF or CH_2Cl_2, yet the highest $^1J(^{77}Se-^{19}F)$ coupling constant in the series is observed for d_8-THF. The trend in coordination effects is consistent with our X-ray studies, where the Se−F and Se−C bond lengths are the shortest in the bis(tetrahydrofuran) adduct of $SeF_2(CN)_2$.

Furthermore, it appears that freezing of the Berry-pseudo-rotation depends not only on temperature but also on the coordination ability of the solvent. Low temperature ^{19}F NMR spectra of $SeF_2(^{13}CN)_2$ in d_5-propionitrile and DME/d_8-toluene exhibit a well-resolved triplet due to coupling of two equatorial ^{13}C nuclei (Berry-pseudo-rotation frozen), whereas solutions in d_8-toluene and CD_2Cl_2 gave only a broad resonance (fast Berry-pseudo-rotation).

Another reason for broad signals in the ^{19}F NMR spectrum is the availability of "free" F^- ions in the solution leading to fast intermolecular exchange as Seppelt stated for SeF_4.[51] Our experiments indicate that this problem occurs in the case of d_8-THF experiments. The cyclic ether can easily be attacked by SeF_4 and related compounds,[52,53] resulting in small but noninnocent amounts of free ions in the solution. "Free" F^- ions can have a serious effect on both the substitution and the decomposition mechanism as they offer alternative pathways via $[SeF_x(CN)_{5-x}]^-$ anions.

Neutral and Anionic Decomposition Pathways for $SeF_x(CN)_{4-x}$ Complexes. Although we carried out low temperature experiments very carefully, hoping that coordinating solvents would stabilize $Se(CN)_4$, the compound remained elusive. Therefore, we carried out extensive DFT calculations to understand the underlying reasons. We determined gas phase reaction energies, a possible CN substitution mechanism, and elimination pathways for selenium(IV) compounds, as well as solvation energies and solvent influence on the decomposition pathways. In addition, we clarify the role of fluoride traces.

Gas Phase Reaction Energies and Elimination TSs in Neutral Se(IV) Compounds. As can be seen in Scheme 3, the first three CN substitutions are moderately to strongly exergonic (~5−13 kcal/mol, gas phase model); however, the final substitution is almost thermoneutral (−0.7 kcal/mol).

Scheme 3. Calculated Gibbs Free Reaction Energies (in kcal/mol) for the Subsequent Substitution of Fluoride with Cyanide[a]

$$SeF_4 + TMSCN \xrightarrow{-8.9/-9.4/\mathbf{-10.6}} SeF_3CN + TMSF$$

$$SeF_3CN + TMSCN \xrightarrow{-12.9/-13.7/\mathbf{-14.9}} SeF_2(CN)_2 + TMSF$$

$$SeF_2(CN)_2 + TMSCN \xrightarrow{-5.5/-8.2/\mathbf{-7.7}} SeF(CN)_3 + TMSF$$

$$SeF(CN)_3 + TMSCN \xrightarrow{-0.7/-2.9/\mathbf{-3.7}} Se(CN)_4 + TMSF$$

[a]Gas phase/*PCM model*/**gas phase + explicitly modeled DME in coordination sphere**. Level of theory: TPSSh/aug-cc-pVTZ//B3LYP/6-311+G(d,p).

Since the second substitution is more exergonic, in the presence of only 1 equiv of TMSCN (trimethylsilyl cyanide) 0.5 equiv of $SeF_2(CN)_2$ will be produced through CN−F exchange of two SeF_3CN molecules (thermodynamically driven, in line with experiments).

FCN or NCCN elimination from SeF_3CN and $SeF_2(CN)_2$ has high barriers (30−40 kcal/mol) as can be seen in Figure 7.

DOI: 10.1021/acs.inorgchem.5b00107
Inorg. Chem. 2015, 54, 5220−5231

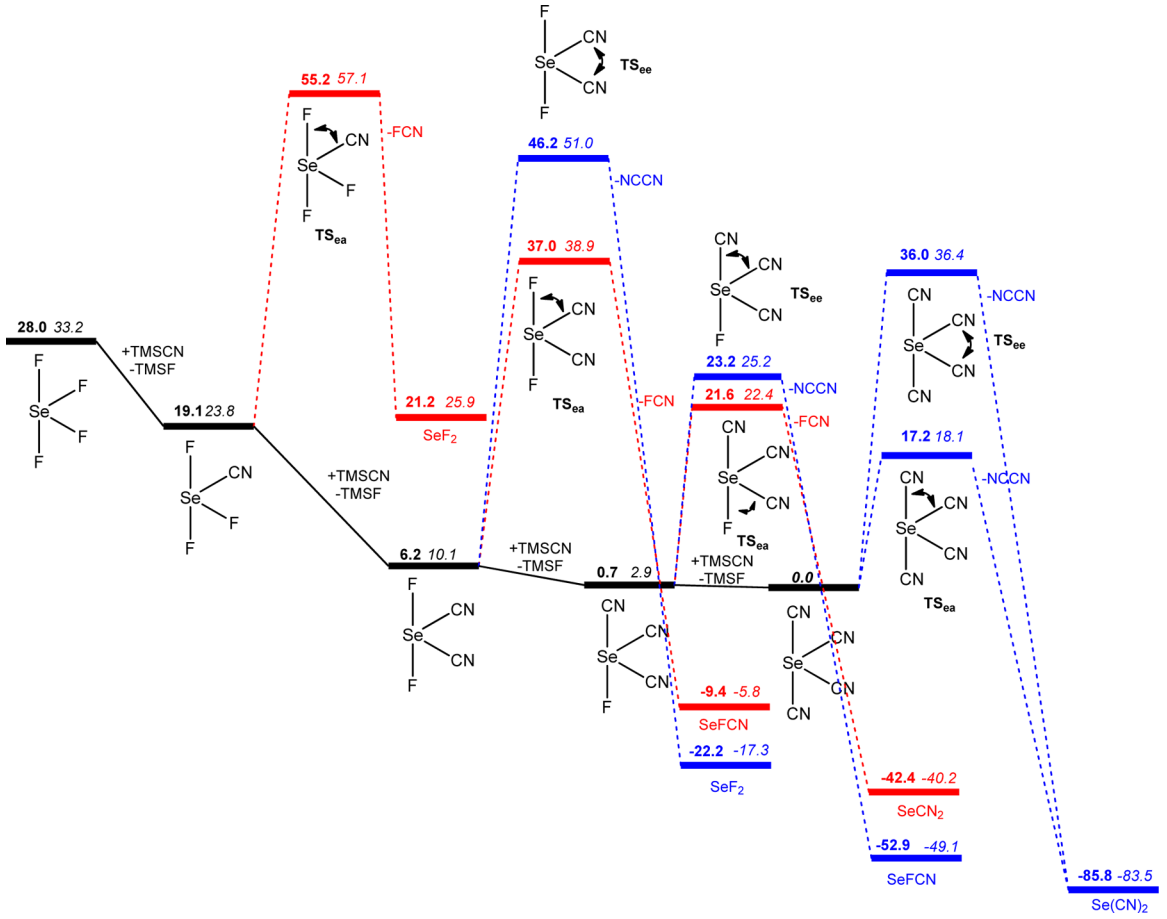

Figure 7. Substitution reactions at Se(IV) and elimination reactions including transition states. Gibbs free energies in gas phase (**bold**, in kcal/mol) and in solution (diethyl ether, PCM model, fully reoptimized, *italic*). TSs and products of FCN elimination in red, of NCCN elimination in blue. To allow incorporation of substitution and decomposition reactions in one figure, all reactions and TSs are reported on the same scale (and referenced to $Se(CN)_4$ + 4 TMSF) by adding the appropriate amount of TMSCN and TMSF molecules with $SeF_x(CN)_{4-x}$ and with TMSCN = 4 − x and TMSF = x. Individual reaction energies and barrier heights are the difference between two structures, e.g., first CN substitution reaction Gibbs free energy, 28.0−19.1 = 8.9 kcal/mol. Level of theory: TPSSh/aug-cc-pVTZ//B3LYP/6-311+G(d,p).

Elimination through an equatorial−apical transition state is always highly preferred (see Figure 8), comparable to the

Figure 8. Equatorial−equatorial (left) vs equatorial−apical elimination transition state in $Se(CN)_4$.

results by Morokuma et al. for SeH_4,[54] and becomes more facile with increasing number of CN substituents. Noticeable is a drop in TS_{eq-ap} energies of the molecules with CN in apical position from 31 kcal/mol for $SeF_2(CN)_2$ to ∼20 kcal/mol for $SeF(CN)_3$ and $Se(CN)_4$. Only $SeF_2(CN)_2$ was experimentally observed. The preference for TS_{eq-ap} is easily rationalized: equatorial bonds of one type are always shorter than apical ones. Shorter bonds have to be stretched more to reach the TS geometry, and the distortion energy necessary to reach the TS geometry will significantly increase the TS energy.

Elimination of FCN from $SeF(CN)_3$ is predicted to be easier than elimination of NCCN. The observation of NCCN in the decomposition reactions can have two reasons: (1) in experiments with excess of TMSCN, FCN can react with it yielding TMSF and NCCN, and (2) $SeF(CN)_3$ can react with excess TMSCN before it decomposes. Either way, already $SeF(CN)_3$ appears to be too unstable to allow for successful isolation.

Solvent Influence on Reaction Energies and Elimination TSs. Polar aprotic solvents have negligible influence on the barrier heights (Figure 7) but influence the reaction energies (Scheme 3). Intermediates and corresponding transition states are similarly elevated in energy; however, substitution reaction energies become slightly more exergonic due to stronger donor coordination with increasing CN content of the molecule as mentioned earlier. These findings are in line with the rather moderate coordination energies of donors in $SeF_x(CN)_{4-x}$ complexes.

We decide to explicitly model the solvent influence on NCCN elimination from $Se(CN)_4$ by including one DME molecule in the first coordination sphere of selenium (Figure 9). However, as the PCM calculations already indicated, solvent influence is only marginal (barrier height in the gas phase 17.2 kcal/mol, in diethyl ether (PCM) 18.1 kcal/mol, with explicitly modeled solvent 17.4 kcal/mol). Therefore, we did not calculate full models (with two DME molecules in the

DOI: 10.1021/acs.inorgchem.5b00107
Inorg. Chem. 2015, 54, 5220−5231

Figure 9. Calculated NCCN elimination TS in $Se(CN)_4$ with coordinated solvent molecule.

coordination sphere of selenium). Similarly, gas phase reaction energies with explicitly modeled solvent molecules in the first coordination sphere (Scheme 3, bold values) are in line with PCM model predictions.

It appears that coordination of solvent molecules does not stabilize the compound with respect to decomposition reactions. Isolation of $Te(CN)_4$ was successfully performed using the stabilizing ability of donating solvents. However, tellurium has the stronger secondary bonding interactions,[48] and differences in reactivity of tellurium(IV) compared to selenium(IV) pseudohalogens can arise from this.

Role of HF Traces in the Substitution and Decomposition Mechanisms. As stated earlier, SeF_4 contains traces of HF. Furthermore, reaction of SeF_4 with solvent molecules can lead to trace amounts of fluoride ions, which are much harder to remove from the SeF_4 than they are from SF_4.[51] Experimentally, free HF or "F^-" should be quickly removed by the (large) excess of TMSCN. This in turn leads to trace amounts of CN^- ions. Depending on the coordination strength of donor solvents like THF or ethers, CN^- or F^- will not be distinct ions but rather bind to $SeF_x(CN)_{4-x}$ forming pentacoordinated selenates. Table 5 shows the gas phase and solvent corrected selenate formation energies from $SeF_x(CN)_{4-x}$ and F^- and CN^-, respectively.[55] While there is no clear trend observable in selenate formation energies with respect to fluorine content, it becomes clear that in solution the energies are significantly smaller.

Furthermore, formation of $[SeF_x(CN)_{5-x}]^-$ is significantly less exergonic if cyanide ions are involved instead of fluoride ions. A strongly coordinating solvent as well as a noncoordinating solvent can neglect the role anions play in substitution and decomposition mechanisms, the former by making the $[SeF_x(CN)_{5-x}]^-$ formation energetically unfavorable (through stronger coordination), the latter by the lack of solubility of the salts.

Comparison of the Gibbs free energies of activation for FCN elimination via an equatorial−apical TS in the neutral $SeF_x(CN)_{4-x}$ and a similar TS in the anionic selenates (Figure 10) shows that formation of selenates lowers the barriers for

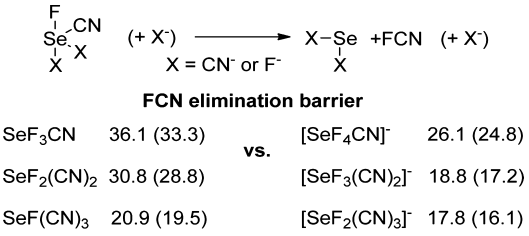

Figure 10. Comparison of Gibbs free energies of activation (in kcal/mol) for FCN elimination in neutral (left) and anionic (right) Se(IV) compounds (we only considered elimination from the most stable $[SeF_x(CN)_{5-x}]^-$ isomer).[55] Level of theory: TPSSh/aug-cc-pVTZ//B3LYP/6-311+G(d,p), values in brackets include PCM (diethyl ether) solvent correction.

decomposition significantly (by ∼3−10 kcal/mol). We tentatively conclude that HF traces can significantly hamper the attempt to isolate $Se(CN)_4$.

CN Substitution Mechanism in the Absence of Anions. In the presence of small amounts of fluoride or cyanide ions, the substitution mechanism is likely to be almost barrierless and involves the stripping of fluorides from $[SeF_x(CN)_{5-x}]^-$ with TMCN via an S_N2-like mechanism followed by quick release of $SeF_x(CN)_{4-x}$ and CN^- (Scheme 4).

Scheme 4. Two-Step Mechanism for CN Substitution in the Presence of Anions

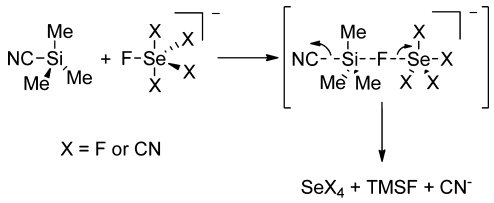

However, in the absence of anions or in noncoordinating solvents like toluene (with sufficiently low anion concentrations) this mechanism is not feasible. Figure 11 shows a plausible mechanism for the CN^- reaction mechanism under these circumstances. We considered σ-metathesis or F-migration followed by elimination to play a role.

CN substitution with THSCN (trihydrosilyl cyanide) via σ-metathesis is considerably easier to achieve than fluorine

Table 5. Calculated Anion Formation Energies (in kcal/mol)

	gas phase				
	ΔE^a	ΔH^a	ΔG^a	ΔG^b	solv^c ΔG^b
	Formation of $[SeF_4CN]^-$ (CN and LP *trans*)				
formation from $SeF_3CN + F^-$	−84.0	−83.7	−75.4	−71.5	−41.8
formation from $SeF_4 + CN^-$	−60.3	−59.2	−49.5	−39.8	−25.9
	Formation of $[SeF_3(CN)_2]^-$ [*mer* (CN−CN−LP) Isomer]				
formation from $SeF_2(CN)_2 + F^-$	−77.2	−76.9	−69.4	−75.1	−32.7
formation from $SeF_3CN + CN^-$	−57.7	−56.6	−46.8	−51.4	−21.4
	Formation of $[SeF_2(CN)_3]^-$ (*fac* F−LP−F Isomer)				
formation from $SeF(CN)_3 + F^-$	−83.3	−83.1	−75.1	−85.0	−38.9
formation from $SeF_2(CN)_2 + CN^-$	−52.8	−51.8	−42.5	−52.1	−20.2

[a]B3LYP. [b]TPSSh. [c]Solvent = diethyl ether (PCM model).

DOI: 10.1021/acs.inorgchem.5b00107
Inorg. Chem. 2015, 54, 5220−5231

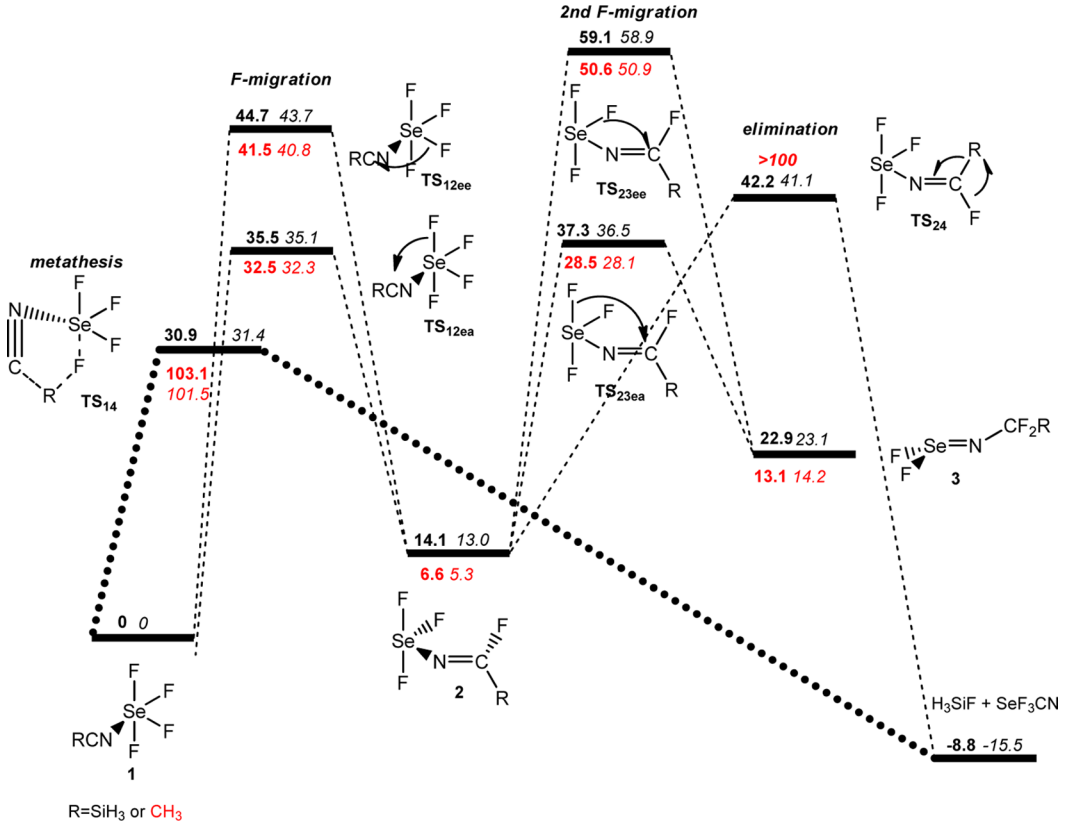

Figure 11. Barrier heights for reactions in neutral Se(IV) compounds. Gibbs free energies in kcal/mol. Level of theory: TPSSh/aug-cc-pVTZ//B3LYP/6-311+G(d,p). Reaction with H_3SiCN (black) and H_3CCN (red). The bold numbers are calculated values in the gas phase, and the italic numbers represent values in diethyl ether.

migration (+5 kcal/mol) followed by elimination (+7 kcal/mol). While the σ-metathesis barrier is smaller than decomposition barriers for SeF_3CN (and although not explicitly shown here supposedly for $SeF_2(CN)_2$), it is higher than decomposition barriers in $SeF(CN)_3$ or $Se(CN)_4$. This is in line with experiments in toluene (very slow formation of $SeF_2(CN)_2$). Note that σ-metathesis yields the isocyanide. However, $SeF_x(CN)_{4-x}$ species in solution are weakly associated, and rapid exchange between two molecules leads to the cyanide.

Thus, in nonpolar solvents, substitution happens via σ-metathesis (not F-migration), but metathesis has a high barrier. Ultimately, the substitution barrier becomes higher than the decomposition barrier; subsequently, isolation of $Se(CN)_4$ is impossible. In polar solvents, in line with experiments, an almost barrierless S_N2-type substitution is possible, but decomposition barriers are also significantly lowered. Unlike in transition metal chemistry, isocyanide σ-metathesis does not play a crucial role in the substitution mechanism.[56,57]

Finally, while THSCN prefers σ-metathesis, this is not possible anymore for H_3CCN, for two reasons: (1) shorter C—C compared to the C—Si bond which makes the required transition state more distorted and (2) lower C—F compared to the Si—F bond energy. Thus, solvent activation of nitriles like propionitrile happens through a series of F-migrations, ultimately yielding $F_2Se{=}N{-}CF_2R$, but it requires significantly higher reaction temperatures. Note that the migration pathway is also significantly easier for CH_3 than it is for SiH_3. Again, all barriers are in principle insensitive to solvent coordination. In line with the calculations, reactions in propionitrile produce significantly smaller amounts of unidentified side products.

Decomposition: Trifluoromethyliminoseleniumdifluoride and a σ-Hole $Se^{II}(CN)_2$ Complex. The above presented neutral decomposition pathways are further justified by the observation of an unknown decomposition product, which is present in tiny amounts when an excess of TMSCN is used but can also be cleanly synthesized when substoichiometric amounts of TMSCN are used. NMR data and quantum mechanical calculations support the identification of the unknown compound as $F_2Se{=}N{-}CF_3$ (Scheme 5).

Scheme 5. Trifluoromethyliminoseleniumdifluoride

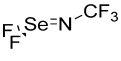

Trifluoromethyliminoseleniumdifluoride was identified by its NMR spectra (Table 6, Figure 12, Supporting Information Figures 1 and 2). Use of ^{13}C-labeled cyanide leads to a quartet signal at 124 ppm in the ^{13}C NMR spectrum due to coupling to three fluorine atoms. The ^{77}Se NMR spectrum (Figure 12) shows a triplet with a large coupling constant arising from the two fluorine atoms bound directly to selenium while the doublet−quartet coupling originating from the $^{13}CF_3$ group collapses to a multiplet. Two signals are present in the ^{19}F NMR spectrum: the doublet at lower frequency is typical for a ^{13}C-labeled $^{13}CF_3$ group, the singlet at higher frequency with ^{77}Se satellites shifts upfield by approximately 50 ppm compared to the analogous sulfur compound. This pronounced difference is common in chalcogen fluorine chemistry. For example, axial

DOI: 10.1021/acs.inorgchem.5b00107
Inorg. Chem. 2015, 54, 5220−5231

Table 6. ^{19}F NMR Data of $F_2Se{=}N{-}^{13}CF_3$ in Comparison with Different Known Imino-Sulfur and Imino-Selenium Compounds[a]

	$\delta(^{19}F)$ (EF_2)	$\delta(^{19}F)$ (CF_3)
$F_2Se{=}N{-}^{13}CF_3$	2.3 ppm (s)	−41.9 ppm (d)
(C_2D_5CN, −80 °C)	$^1J(^{19}F{-}^{77}Se)$ = 692 Hz	$^1J(^{19}F{-}^{13}C)$ = 260 Hz
$F_2Se{=}N{-}^{13}CF_3$	−3.9 ppm (s)	−40.7 ppm (dt)
(DME/C_7D_8, −80 °C)	$^1J(^{19}F{-}^{77}Se)$ = 640 Hz	$^1J(^{19}F{-}^{13}C)$ = 262 Hz
		$^4J(^{19}F{-}^{19}F)$ = 11.6 Hz
$F_2Se{=}N{-}TeF_5$[58]	38.0 ppm (broad)	
	$^1J(^{19}F{-}^{77}Se)$ = 808.4 Hz	
$F_2S{=}N{-}TeF_5$[58]	66.2 ppm	
$F_2S{=}N{-}CF_3$[59]	49.7 ppm (q)	−49.4 ppm (t)
	$^4J(^{19}F{-}^{19}F)$ = 9.8 Hz	$^4J(^{19}F{-}^{19}F)$ = 11.3 Hz

[a]376 MHz, chemical shift referenced to $CFCl_3$.

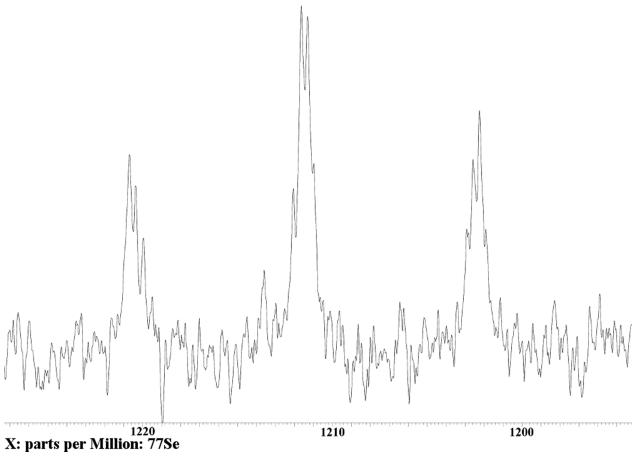

Figure 12. ^{77}Se NMR spectrum of $F_2Se{=}N{-}^{13}CF_3$ (C_2D_5CN, −80 °C, 76 MHz, chemical shift referenced to external Me_2Se).

bound fluorine atoms shift from 88 ppm in SF_4 to 37 ppm in SeF_4.[60] Additionally, ^{19}F NMR chemical shifts in chalcogen chemistry are highly solvent and temperature dependent. A 60 ppm difference from $F_2Se{=}N{-}CF_3$ to $F_2Se{=}N{-}TeF_5$ is not surprising, as the latter was measured neat and at room temperature. The same holds true for the comparison of the coupling constants.

The formation of $F_2Se{=}N{-}CF_3$ starting from FCN and SeF_4 likely occurs analogously to that of $F_2S{=}N{-}CF_3$ published by Sundermeyer and Schachner.[59] NMR spectra confirm that both, FCN and SeF_4, are present during the decomposition but not initially and therefore must be generated in situ. The second main decomposition product is $Se(CN)_2$. Therefore, the decomposition mechanism is proposed as follows.

The most important step is the formation of the trisubstituted $SeF(CN)_3$ which quickly decomposes giving FCN and $Se(CN)_2$ (in line with DFT calculations). An equilibrium between the different $SeF_x(CN)_{4-x}$ (with x = 1−3) species must exist, that also leads to the reformation of SeF_4 (Scheme 6). Direct decomposition of $SeF_2(CN)_2$ does not play a crucial role as it has high barriers and would yield an extremely unstable selenium(II) fluoride species.[61,62]

Using less TMSCN in decomposition experiments (1.5 equiv per SeF_4) results in formation of almost pure $F_2Se{=}N{-}CF_3$. Attempts to obtain $F_2Se{=}N{-}CF_3$ from a reaction of SeF_4 with $(FCN)_3$ and CsF in analogy to the sulfur compound were not successful.[63]

Scheme 6. Decomposition of $SeF_2(CN)_2$

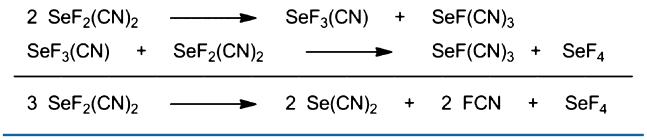

Figure 13 shows the reaction mechanism for the reaction of SeF_4 with FCN in accordance with the mechanism described by

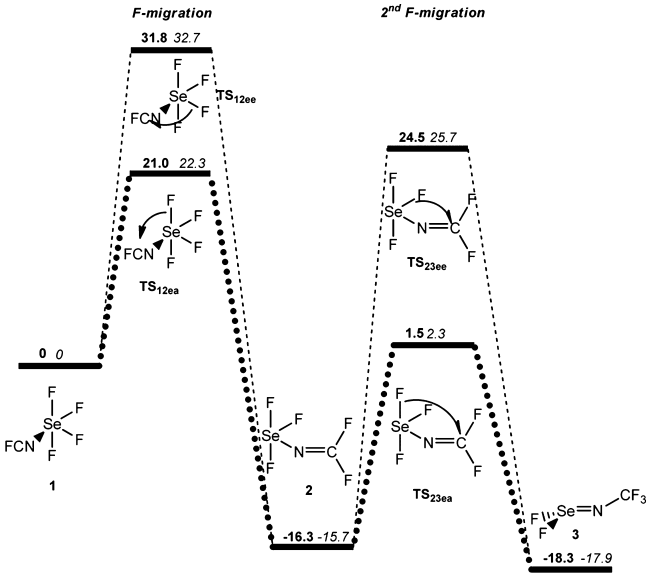

Figure 13. Reaction pathway for the formation of $F_2Se{=}NCF_3$ from SeF_4 and FCN and calculated gas phase Gibbs free energies (in kcal/mol). Level of theory: TPSSh/aug-cc-pVTZ//B3LYP/6-311+G(d,p).

Smith and Tullock for the reaction of SF_4 with nitriles.[64] Reaction of FCN with SeF_4 is predicted to have relatively low barriers (21.0 kcal/mol). The second fluorine migration (**2** to TS_{23ea}) is slightly easier (−3.2 kcal/mol) than the first one (**1** to TS_{12ea}). Therefore, it is unlikely that the intermediate $SeF_3{-}N{=}CF_2$ is generated in noticeable amounts. Equatorial−apical TSs are strongly preferred (10−20 kcal/mol). In summary, NMR data, quantum mechanical calculations, and similarities with sulfur chemistry point to the unknown decomposition product being $F_2Se{=}N{-}CF_3$.

Finally, the other decomposition product, selenium dicyanide, was crystallized as 18-crown-6 adduct, which is monomeric contrary to the already published 1,2-dimethoxy-

DOI: 10.1021/acs.inorgchem.5b00107
Inorg. Chem. 2015, 54, 5220−5231

ethane adduct which forms a solvent-bridged dimer.[11] In comparison to $SeF_2(CN)_2$·18-crown-6, the change in the oxidation state of selenium from IV to II leads to a new coordination motif (Figure 14). $Se(CN)_2$ is coordinated by

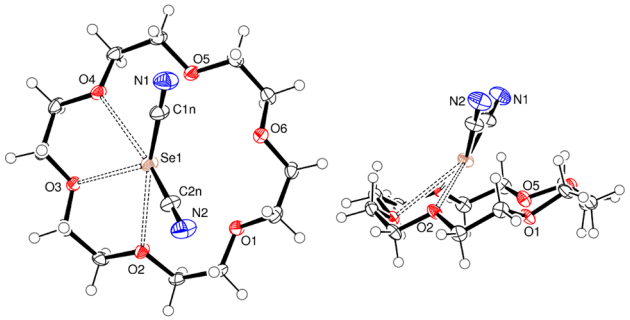

Figure 14. Molecular structure of $Se(CN)_2$·18-crown-6. For clarity, additional cocrystallized 18-crown-6 is not shown. ORTEP[41] drawing with 50% probability ellipsoids.

three oxygen atoms deviating only 13° from the cyanide plane. This is more than in the 1,2-dimethoxyethane adduct where the angle between the (O−Se−O) and (C−Se−C) plane is only 7°. Due to the lower flexibility of the crown ether, Se−O distances are up to 0.24 Å longer than in the 1,2-dimethoxyethane adduct but still distinctly below the sum of the van der Waals radii.[46] These results and the location of the coordination in the extended direction of the selenium cyanide bonds are in line with the σ-hole concept.[65]

4. CONCLUSION

We hypothesized that secondary bonding interactions would stabilize $Se(CN)_4$ similar to $Te(CN)_4$. However, the observed solvent insensitivity of selenium(IV) compounds toward reductive elimination barriers and substitution energies is remarkable and was unexpected. In line with this, secondary bonding interactions in $SeF_2(CN)_2$ donor complexes are rather weak and do not lead to pronounced changes in the observed structure of the $SeF_2(CN)_2$ unit.

Although decomposition barriers for neutral selenium(IV) complexes are considerably higher compared to selenates, so are "substitution" barriers. Substitution in noncoordinating solvents likely happens via σ-metathesis. Previously unknown trifluoromethyliminoseleniumdifluoride has been synthesized, indirectly pointing to the intermediate existence of $SeF(CN)_3$ which decomposes to yield FCN and $Se(CN)_2$. The thermodynamically more favorable NCCN elimination has a higher activation barrier.

The instability of $SeF(CN)_3$ adds another obstacle on the way to obtain $Se(CN)_4$. Ultimately, although earlier experiments indicated that $Se(CN)_4$ can exist (via identification of its decomposition product NCCN), it appears highly unlikely that it can ever be isolated successfully (other than by molecular beam or matrix experiments) as low lying neutral and anionic decomposition pathways exist. Additionally, the final CN substitution is barely exergonic.

■ ASSOCIATED CONTENT

Supporting Information

X-ray crystallographic file in CIF format, table with crystal structure refinement data; tables for final energies and thermochemistry corrections, pictures of ^{13}C and ^{19}F NMR spectra of $F_2Se{=}N^{13}CF_3$, and xyz files for all structures. The Supporting Information is available free of charge on the ACS Publications website at DOI: 10.1021/acs.inorgchem.5b00107.

■ AUTHOR INFORMATION

Corresponding Author

*E-mail: ce.christian.ehm@gmail.com. Phone: +49-30-838-52695. Fax: +49-30-838-53310.

Present Address

†Dipartimento di Scienze Chimiche, Università di Napoli Federico II, Via Cintia, 80126 Napoli, Italy. E-mail: christian.ehm@unina.it. Phone: +39-081-674361. Fax: +39-081-679970.

Author Contributions

The manuscript was written through contributions of all authors. All authors have given approval to the final version of the manuscript.

Notes

The authors declare no competing financial interest.

■ ACKNOWLEDGMENTS

Support from the Center for Supramolecular Interactions of the Freie Universität Berlin is gratefully acknowledged. We appreciate the generous allocation of computational time by the High Performance Computing Group at the ZEDAT of the Freie Universität Berlin. We thank Dr. Justin T. Foy for valuable comments on the manuscript.

■ REFERENCES

(1) Aksnes, O.; Foss, O. *Acta Chem. Scand.* **1954**, *8*, 1787.
(2) Aksnes, O.; Foss, O. *Acta Chem. Scand.* **1954**, *8*, 702.
(3) Birckenbach, L.; Kellermann, K. *Ber. Deut. Chem. Ges. A and B* **1925**, *58*, 786.
(4) Birckenbach, L.; Kellermann, K. *Ber. Deut. Chem. Ges. A and B* **1925**, *58*, 2377.
(5) Burchell, C. J.; Kilian, P.; Slawin, A. M. Z.; Woollins, J. D.; Tersago, K.; Van Alsenoy, C.; Blockhuys, F. *Inorg. Chem.* **2006**, *45*, 710.
(6) Klapötke, T. M.; Krumm, B.; Scherr, M. *Inorg. Chem.* **2008**, *47*, 7025.
(7) Klapötke, T. M.; Krumm, B.; Gálvez-Ruiz, J. C.; Nöth, H.; Schwab, I. *Eur. J. Inorg. Chem.* **2004**, *2004*, 4764.
(8) Maaninen, A.; Chivers, T.; Parvez, M.; Pietikäinen, J.; Laitinen, R. S. *Inorg. Chem.* **1999**, *38*, 4093.
(9) Dutton, J. L.; Tabeshi, R.; Jennings, M. C.; Lough, A. J.; Ragogna, P. J. *Inorg. Chem.* **2007**, *46*, 8594.
(10) Lentz, D.; Szwak, M. *Angew. Chem., Int. Ed.* **2005**, *44*, 5079.
(11) Fritz, S.; Lentz, D.; Szwak, M. *Eur. J. Inorg. Chem.* **2008**, *2008*, 4683.
(12) Jacobs, J.; Willner, H. *Z. Anorg. Allg. Chem.* **1993**, *619*, 1221.
(13) Seppelt, K.; Lentz, D.; Klöter, G.; Schack, C. J. In *Inorganic Syntheses*; John Wiley & Sons, Inc.: Hoboken, NJ, 1986; p 27.
(14) Veith, M.; Bärnighausen, H. *Acta Crystallogr., Sect. B* **1974**, *30*, 1806.
(15) Frisch, M. J.; Trucks, G. W.; Schlegel, H. B.; et al.*Gaussian 09, B.01*; Gaussian, Inc.: Wallingford, CT, 2009. For the complete citation, see the Supporting Information.
(16) Becke, A. D. *Phys. Rev. A* **1988**, *38*, 3098.
(17) Becke, A. D. *J. Chem. Phys.* **1993**, *98*, 1372.
(18) Becke, A. D. *J. Chem. Phys.* **1993**, *98*, 5648.
(19) Stephens, P. J.; Devlin, F. J.; Chabalowski, C. F.; Frisch, M. J. *J. Phys. Chem.* **1994**, *98*, 11623.
(20) Lee, C. T.; Yang, W. T.; Parr, R. G. *Phys. Rev. B* **1988**, *37*, 785.
(21) Zhao, Y.; Truhlar, D. G. *Theor. Chem. Acc.* **2008**, *120*, 215.
(22) Tao, J. M.; Perdew, J. P.; Staroverov, V. N.; Scuseria, G. E. *Phys. Rev. Lett.* **2003**, *91*, 146401.

DOI: 10.1021/acs.inorgchem.5b00107
Inorg. Chem. 2015, 54, 5220−5231

(23) Dunning, T. H. *J. Chem. Phys.* **1989**, *90*, 1007.
(24) Kendall, R. A.; Dunning, T. H.; Harrison, R. J. *J. Chem. Phys.* **1992**, *96*, 6796.
(25) Woon, D. E.; Dunning, T. H. *J. Chem. Phys.* **1995**, *103*, 4572.
(26) Peterson, K. A.; Dunning, T. H. *J. Chem. Phys.* **2002**, *117*, 10548.
(27) Woon, D. E.; Dunning, T. H. *J. Chem. Phys.* **1993**, *98*, 1358.
(28) Wilson, A. K.; Woon, D. E.; Peterson, K. A.; Dunning, T. H. *J. Chem. Phys.* **1999**, *110*, 7667.
(29) Peterson, K. A.; Yousaf, K. E. *J. Chem. Phys.* **2010**, *133*, 174116.
(30) See http://tyr0.chem.wsu.edu/~kipeters/basis-bib.html for a bibliography of correlation consistent basis sets.
(31) Feller, D. *J. Comput. Chem.* **1996**, *17*, 1571.
(32) Schuchardt, K. L.; Didier, B. T.; Elsethagen, T.; Sun, L. S.; Gurumoorthi, V.; Chase, J.; Li, J.; Windus, T. L. *J. Chem. Inf. Model.* **2007**, *47*, 1045.
(33) Grimme, S.; Ehrlich, S.; Goerigk, L. *J. Comput. Chem.* **2011**, *32*, 1456.
(34) Grimme, S.; Antony, J.; Ehrlich, S.; Krieg, H. *J. Chem. Phys.* **2010**, *132*, 154104.
(35) Ehm, C.; Budzelaar, P. H. M.; Busico, V. *J. Organomet. Chem.* **2015**, *775*, 39.
(36) The Berny algorithm was never completely published; see the Gaussian documentation for details.
(37) Peng, C. Y.; Ayala, P. Y.; Schlegel, H. B.; Frisch, M. J. *J. Comput. Chem.* **1996**, *17*, 49.
(38) Peng, C. Y.; Schlegel, H. B. *Isr. J. Chem.* **1993**, *33*, 449.
(39) Boys, S. F.; Bernardi, F. *Mol. Phys.* **1970**, *19*, 553.
(40) Tomasi, J.; Mennucci, B.; Cammi, R. *Chem. Rev.* **2005**, *105*, 2999.
(41) Farrugia, L. *J. Appl. Crystallogr.* **1997**, *30*, 565.
(42) Baxter, P. L.; Downs, A. J.; Forster, A. M.; Goode, M. J.; Rankin, D. W. H.; Robertson, H. E. *J. Chem. Soc., Dalton Trans.* **1985**, 941.
(43) Kniep, R.; Korte, L.; Kryschi, R.; Poll, W. *Angew. Chem., Int. Ed. Engl.* **1984**, *23*, 388.
(44) Kniep, R.; Korte, L.; Kryschi, R.; Poll, W. *Angew. Chem.* **1984**, *96*, 351.
(45) Bowater, I. C.; Brown, R. D.; Burden, F. R. *J. Mol. Spectrosc.* **1968**, *28*, 454.
(46) Bondi, A. *J. Phys. Chem.* **1964**, *68*, 441.
(47) Picture was created using data from ref 11/CCDC-695320.
(48) Panda, A.; Behera, R. N. *J. Hazard. Mater.* **2014**, *269*, 2.
(49) Shargi, S. N.; Webb, G. A. *Org. Magn. Reson.* **1982**, *19*, 216.
(50) Gillespie, R. J.; Schrobilgen, G. J. *Inorg. Chem.* **1974**, *13*, 765.
(51) Seppelt, K. *Z. Anorg. Allg. Chem.* **1975**, *416*, 12.
(52) Wang, C.-L. J. In *Organic Reactions*; John Wiley & Sons, Inc.: New York, 2004.
(53) Olah, G. A.; Nojima, M.; Kerekes, I. *J. Am. Chem. Soc.* **1974**, *96*, 925.
(54) Moc, J.; Dorigo, A. E.; Morokuma, K. *Chem. Phys. Lett.* **1993**, *204*, 65.
(55) Only the most stable isomer of the Ψ-octahedral selenates is shown (out of two for $[SeF_4CN]^-$, and three each for $[SeF_3(CN)_2]^-$ and $[SeF_2(CN)_3]^-$). In accordance with VSEPR predictions, in all cases the isomer with CN^- and the lone pair trans to each other is the most stable.
(56) Treichel, P. M.; Shaw, D. B. *J. Organomet. Chem.* **1977**, *139*, 21.
(57) Nitriles like THSCN always contain small amounts of the less stable isocyanide which can yield more stable complexes, as observed for example with Cr, Mo, and W carbonyls. However, coordination of both THSCN and THSNC to SeF_4 is slightly endergonic (4.1 vs 1.7 kcal/mol), and the associated isocyanide σ-metathesis TS is overall higher in Gibbs free energy (31.3 vs 35.5 kcal/mol).
(58) Hartl, H.; Huppmann, P.; Lentz, D.; Seppelt, K. *Inorg. Chem.* **1983**, *22*, 2183.
(59) Schachner, H.; Sundermeyer, W. *J. Fluorine Chem.* **1981**, *18*, 259.
(60) Berger, S.; Braun, S.; Kalinowski, H.-O. *19 F-NMR-Spektroskopie*; Georg Thieme Verlag: Stuttgart, 1994.
(61) Poleschner, H.; Ellrodt, S.; Malischewski, M.; Nakatsuji, J.-y.; Rohner, C.; Seppelt, K. *Angew. Chem., Int. Ed.* **2012**, *51*, 419.
(62) Haas, A. *J. Fluorine Chem.* **1986**, *32*, 415.
(63) Griffiths, J. E.; Sturman, D. F. *Spectrochim. Acta, Part A* **1969**, *25*, 1355.
(64) Smith, W. C.; Tullock, C. W.; Smith, R. D.; Engelhardt, V. A. *J. Am. Chem. Soc.* **1960**, *82*, 551.
(65) Murray, J.; Lane, P.; Clark, T.; Politzer, P. *J. Mol. Model.* **2007**, *13*, 1033.

DOI: 10.1021/acs.inorgchem.5b00107
Inorg. Chem. 2015, 54, 5220−5231